

# Modeling and Control of Offshore Pipelay Operations Based on a Finite Strain Pipe Model

Gullik A. Jensen, Niklas Säfström, Tu Duc Nguyen and Thor I. Fossen

**Abstract**—This paper deals with modeling and control of offshore pipelay operations from a dynamically positioned surface vessel where a nonlinear dynamic beam formulation in three dimensions capable of undergoing shearing, twist and bending is used to model the pipe. This pipe model is coupled with a nonlinear vessel model that has been adopted as a standard for vessel control design and analysis purposes. The complete pipelay system is shown to be input-output passive taking the thruster force as the input and the vessel velocity as the output. A nonlinear controller is applied, and using the passivity condition of feedback connection of two passive systems, the closed loop system is stable. Numerical simulations using both PD and PID controllers illustrate the theoretical results.

## I. INTRODUCTION

Over the last decade deepwater pipelaying has gone through a spectacular development. In the early 90s a water depth of 300 meters was considered deep, while today depths of 2000 meters are common practice. The unprecedented global demand for oil and gas is the main drive in the offshore petroleum industry, which in turn demands improved pipeline technology. The installation of pipelines and flowlines constitute some of the most challenging offshore operations handled, and the required engineering sophistication, as well as the size and complexity of the vessels used, has developed pipelaying into an engineering discipline of its own accord [13]. Present trends in the marked increase in deepwater projects as well in length as depth, according to [12].

Purpose built pipelay vessels equipped with dynamic positioning systems are used for installation of offshore pipelines. The pipe is clamped on to the vessel by heavy tension equipment and extended in a production line accommodating either S-lay or J-lay, which are the two main pipelay methods. The S-lay method is fast and economical and dominates the pipelay market. The pipe is extended horizontally and it describes an S-shaped curve to the seabed, see Figure 1. The upper part (*overbend*) is supported by a submerged supporting structure called a *stinger* to control curvature and ovalization, and the curvature in the lower curve (*sagbend*) is controlled by pipe tension. The strain

must be checked against pipe design parameters to stay within limits for buckling and ovalization. In deep waters, the weight of the pipe makes it difficult to maintain a stinger supported overbend due to the increased pipe tension, but the tension may be reduced by adopting the J-lay method where the pipe is extended near vertically and thus eliminates the overbend. The methods are seen to be complementary [15]. Both methods are well described in recent textbooks such as [2], [7] and [14]. The present trends in deepwater pipelay systems are described in [8] and the references therein.

Mathematical models are vital in pipeline design for analysis of pipelay parameters and for operability analysis. Commercially developed computer tools, e.g., OFFPIPE, RIFLEX and SIMLA, that are based on *finite element* models has become the universal method for modeling pipelay operations in the industry. These models capture well the dynamics of the pipe and has replaced simpler models, e.g., the static catenary model and stiffened catenary model [3], [16], which was exploited in earlier years. These finite element models are not suited in model-based controllers for pipelay operations, as the system may become unstable due to unmodeled system modes, the so-called *spillover* [1], since the passivity analysis is performed on a finite-dimensional model rather than an infinite-dimensional model.

In this paper a mathematical model for the dynamics of pipelay operations are developed, limited to a surface vessel and pipe where the pipe is clamped to the vessel at an arbitrary angle. The pipe dynamics are modeled by a three dimensional finite strain beam formulation obtained from the classical study of rods. This is a geometrically correct model of nonlinear rods capable of undergoing finite extension, shearing, twist and bending. The key feature of this model is the choice of parametrization which yields the momentum equation on a form which strongly resembles the classical Euler equation of rigid body dynamics, and it is well suited for both mathematical and numerical analysis.

A vessel model on vectorial form using Euler angles is used here since Euler angles are preferred for quantifying attitude in marine applications, despite the singularity issue. The models are coupled by applying the vessel as a boundary condition of the partial differential equation describing the pipe. The system is shown to be input-output passive when the vessel thruster forces are taken as input and the vessel velocity is taken as the output. Hence, stability of the closed loop system follows for a passive controller. Numerical simulations are provided to illustrate the theoretical results.

G. A. Jensen and T. I. Fossen are with Department of Engineering Cybernetics, and Centre for Ships and Ocean Structures, Norwegian University of Science and Technology, Trondheim, Norway [gullik.jensen@itk.ntnu.no](mailto:gullik.jensen@itk.ntnu.no), [fossen@ieee.org](mailto:fossen@ieee.org)

N. Säfström is with Department of Mathematical Sciences, Norwegian University of Science and Technology, Trondheim, Norway [savstrom@math.ntnu.no](mailto:savstrom@math.ntnu.no)

T.D. Nguyen is with Siemens Oil & Gas Offshore, Trondheim, Norway [tu.nguyen@siemens.com](mailto:tu.nguyen@siemens.com)

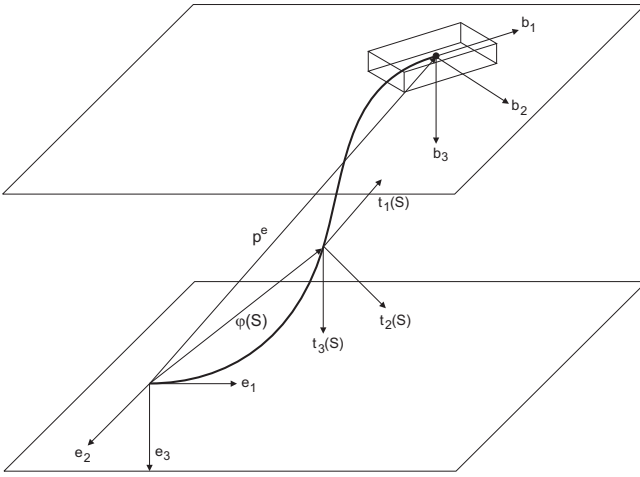


Fig. 1. A schematic presentation of the pipe and vessel system in a S-lay configuration shown in three degrees of freedom. All the coordinate frames used are shown.

## II. MATHEMATICAL MODEL

In this section the mathematical model is developed for the system of a surface vessel with a freely suspended slender pipe string extending from the vessel at a touchdown point at the seabed, see Figure 1. The model of the vessel is the familiar system of ordinary differential equations on vectorial form, as presented in [5], and the pipe model is a nonlinear partial differential equation presented in [9], which extends the finite strain beam theory presented by Simo et. al in [17], [18], [19], [20], to apply for a pipeline submerged in a fluid by adding hydrodynamic and hydrostatic effects. The configurations of the pipe are completely defined by specifying the evolution of an orthogonal matrix, and position vector of line of centroids [17].

### A. Notation

Vectors are represented with bold face lower case letters, while bold face upper case letters denote matrices. All vectors are given as coordinate vectors with reference to a frame which is indicated by a superscript, which may be omitted if the frame dependency is evident. A superposed dot denotes the derivative with respect to time, and a prefixed  $\partial_S$  indicates the material derivative. The usual inner product is equally defined by  $\langle \mathbf{a}, \mathbf{b} \rangle$  and  $\mathbf{a}^T \mathbf{b}$  for all  $\mathbf{a}, \mathbf{b} \in \mathbb{R}^n$ .

### B. Kinematics

The pipe is in a classical point of view a rod, which is a three-dimensional body whose reference configuration can be described by a smooth curve  $\varphi_0$ , where planes called *cross-sections* are attached at each point of  $\varphi_0$ . The curve  $\partial_S \varphi_0$  is assumed to be normal to the plane of each cross-section and intersecting the plane at the centroid. Any configuration of the pipe is thus given by a smooth curve  $\varphi : [0, L] \rightarrow \mathbb{R}^3$  denoted the *line of centroids*, where  $L$  is the total length of  $\varphi_0$ , and thus the undeformed pipe. The cross-sections are assumed to remain unchanged in shape but not necessarily remain normal to  $\partial_S \varphi$  while the pipe is undergoing motion,

which means that the pipe model is capable of undergoing shearing. The outlined kinematic model is known as the constrained two director *Cosserat rod*.

Let  $\mathbf{t}$  be an orthonormal frame with base  $\mathbf{t}_1, \mathbf{t}_2, \mathbf{t}_3$  with  $\mathbf{t}_2$  and  $\mathbf{t}_3$  directed along the principal axis of the plane and  $\mathbf{t}_1$  normal to the plane in order to form a right-hand system, with the origin  $O_t$  at the centroid. In rigid body mechanics the frame  $\mathbf{t}$  is called a *body frame*. Let  $\mathbf{e}$  be an inertial frame with orthonormal base  $\mathbf{e}_1, \mathbf{e}_2, \mathbf{e}_3$  and origin  $O_e$  located at the pipe touchdown point fixed on the sea floor. The orientation of  $\mathbf{t}$  along  $\varphi(S)$  relative to  $\mathbf{e}$  is given by the rotation matrix  $\mathbf{R}_t^e : [0, L] \rightarrow \text{SO}(3)$ , where  $\text{SO}(3) \subset \mathbb{R}^3$  denotes the *special orthogonal group* of order three, such that for  $i = 1, 2, 3$ ,

$$\mathbf{t}_i^e = \mathbf{R}_t^e \mathbf{e}_i^e. \quad (1)$$

The velocity of the points of  $\varphi(S, t)$  is given as  $\dot{\varphi}(S, t)$ , and the spatial angular velocity of frame  $\mathbf{t}$  is given as

$$\dot{\mathbf{R}}_t^e = (\mathbf{w}^e)^\times \mathbf{R}_t^e, \quad (2)$$

where  $(\cdot)^\times$  is the skew-symmetric operator, and  $(\mathbf{w}^e)^\times$  is the *vorticity* in the inertial frame. The associated vector  $\mathbf{w}^e \in \mathbb{R}^3$  is the spatial angular velocity of the cross-sections.

Marine vessels moving in six degrees of freedom (DOF) requires a minimum of six independent coordinates to uniquely determine position and orientation. Let  $\mathbf{b}$  be a body fixed frame with the origin  $O_b$  located at the center of gravity of the pipelay vessel and orthonormal base  $\mathbf{b}_1, \mathbf{b}_2, \mathbf{b}_3$  directed along the principal axes of symmetry of the vessel. Let the generalized position and orientation of the vessel be given as

$$\boldsymbol{\eta}^e = [ \mathbf{p}^T \quad \boldsymbol{\Theta}^T ]^T \in \mathbb{R}^6, \quad (3)$$

where  $\mathbf{p} = [x, y, z]^T$  is the position in the  $\mathbf{e}$  frame, and  $\boldsymbol{\Theta} = [\phi, \theta, \psi]^T$  representing the orientation  $\mathbf{R}_t^e$  in Euler angles by the *zyx*-convention. The velocity of the vessel  $\boldsymbol{\nu}^b$ , is expressed in the body-fixed frame  $\mathbf{b}$  such that

$$\boldsymbol{\nu}^b = [ \mathbf{v}^T \quad \boldsymbol{\omega}^T ]^T \in \mathbb{R}^6. \quad (4)$$

where  $\mathbf{v} \in \mathbb{R}^3$  represents the linear velocity, and  $\boldsymbol{\omega} \in \mathbb{R}^3$  represents the angular velocity. Let the pipe be clamped to the vessel such that  $O_b$  coincides with  $O_t$  at  $S = L$ , at an arbitrary fixed angle  $\beta$ . The rotation matrix  $\mathbf{R}_b^e$ , rotating from  $\mathbf{e}$  to  $\mathbf{b}$  is

$$\mathbf{R}_b^e = \mathbf{R}_t^e(L) \mathbf{R}_b^t(\beta), \quad (5)$$

where  $\mathbf{R}_b^t$  is a constant. The mapping of velocity between the frame  $\mathbf{e}$ -frame and the  $\mathbf{b}$ -frame is

$$\dot{\boldsymbol{\eta}}^e = \mathbf{J}(\boldsymbol{\eta}^e) \boldsymbol{\nu}^b, \quad (6)$$

where  $\mathbf{J}(\boldsymbol{\eta}^e) \in \mathbb{R}^{6 \times 6}$  is found as

$$\mathbf{J}(\boldsymbol{\eta}^e) = \begin{bmatrix} \mathbf{R}_b^e & \mathbf{0}_{3 \times 3} \\ \mathbf{0}_{3 \times 3} & \boldsymbol{\Pi}_e^{-1} \mathbf{R}_b^e \end{bmatrix} \in \mathbb{R}^{6 \times 6}, \quad \theta \neq \pm \frac{\pi}{2}. \quad (7)$$

The mapping  $\boldsymbol{\Pi}_e$  between angular velocity  $\mathbf{w}^e$  and the rate of change of the Euler angles  $\dot{\boldsymbol{\Theta}}$  is developed by manipulating equation (2), such that

$$\mathbf{w}^e = \boldsymbol{\Pi}_e \dot{\boldsymbol{\Theta}} \quad (8)$$

where

$$\mathbf{\Pi}_e(\Theta) = \begin{bmatrix} \cos \theta \cos \psi & -\sin \psi & 0 \\ \cos \theta \sin \psi & \cos \psi & 0 \\ -\sin \theta & 0 & 1 \end{bmatrix}. \quad (9)$$

This parametrization of the rotation with respect to Euler angles by the  $zyx$ -convention introduces a singularity in pitch for the inverse kinematics. Alternative conventions can be applied to move the singularity, or it can be removed completely by using quaternions.

The superscripts of  $\boldsymbol{\eta}^e$  and  $\boldsymbol{\nu}^b$  will be omitted for the remainder of this paper.

### C. The Vessel Dynamics

The equations of motion of a marine vessel given in the body frame is known from [5] as

$$\mathbf{M}\dot{\boldsymbol{\nu}} + \mathbf{C}(\boldsymbol{\nu})\boldsymbol{\nu} + \mathbf{D}(\boldsymbol{\nu})\boldsymbol{\nu} + \mathbf{g}(\boldsymbol{\eta}) = \boldsymbol{\tau} + \boldsymbol{\chi} + \mathbf{w} \quad (10)$$

where

- $\mathbf{M}$  - system inertia matrix
- $\mathbf{C}(\boldsymbol{\nu})$  - Coriolis-centripetal matrix
- $\mathbf{D}(\boldsymbol{\nu})$  - damping matrix
- $\mathbf{g}(\boldsymbol{\eta})$  - vector of restoring forces and moments
- $\boldsymbol{\tau}$  - vector of control inputs
- $\boldsymbol{\chi}$  - vector of forces and moments from the pipe
- $\mathbf{w}$  - vector of environmental forces

where  $\mathbf{M}$  is symmetric positive definite,  $\mathbf{C}(\boldsymbol{\nu})$  is skew-symmetrical and  $\mathbf{D}(\boldsymbol{\nu})$  is positive definite. Expressing the equation of motion in the inertial frame  $\mathbf{e}$  is found by substituting (6) into (10) such that

$$\begin{aligned} \mathbf{M}_\eta(\boldsymbol{\eta})\dot{\boldsymbol{\eta}} + \mathbf{C}_\eta(\boldsymbol{\nu}, \boldsymbol{\eta})\dot{\boldsymbol{\eta}} + \mathbf{D}_\eta(\boldsymbol{\nu}, \boldsymbol{\eta})\dot{\boldsymbol{\eta}} + \mathbf{g}_\eta(\boldsymbol{\eta}) \\ = \mathbf{J}^{-T}(\boldsymbol{\eta})\boldsymbol{\tau} + \mathbf{J}^{-T}(\boldsymbol{\eta})\boldsymbol{\chi} \end{aligned} \quad (11)$$

where

$$\mathbf{M}_\eta(\boldsymbol{\eta}) = \mathbf{J}^{-T}\mathbf{M}\mathbf{J}^{-1} \quad (12)$$

$$\mathbf{C}_\eta(\boldsymbol{\nu}, \boldsymbol{\eta}) = \mathbf{J}^{-T} \left[ \mathbf{C}(\boldsymbol{\nu}) - \mathbf{M}\mathbf{J}^{-1}\dot{\mathbf{J}} \right] \mathbf{J}^{-1} \quad (13)$$

$$\mathbf{D}_\eta(\boldsymbol{\nu}, \boldsymbol{\eta}) = \mathbf{J}^{-T}\mathbf{D}(\boldsymbol{\nu})\mathbf{J}^{-1} \quad (14)$$

$$\mathbf{g}_\eta(\boldsymbol{\eta}) = \mathbf{J}^{-T}\mathbf{g}(\boldsymbol{\eta}) \quad (15)$$

The vector of forces and moments from the pipe  $\boldsymbol{\chi}$ , is presented as the boundary condition for the pipe in the next section. Note that  $\boldsymbol{\chi}$  is given in the body fixed frame of the vessel. For the later passivity analysis the following properties of (11) holds:

- P1)**  $\mathbf{M}_\eta(\boldsymbol{\eta}) = \mathbf{M}_\eta^T(\boldsymbol{\eta}) > 0, \quad \forall \boldsymbol{\eta} \in \mathbb{R}^6$
- P2)**  $\mathbf{s}^T \left[ \dot{\mathbf{M}}_\eta(\boldsymbol{\eta}) - 2\mathbf{C}_\eta(\boldsymbol{\nu}, \boldsymbol{\eta}) \right] \mathbf{s} = 0, \quad \forall \mathbf{s}, \boldsymbol{\nu}, \boldsymbol{\eta} \in \mathbb{R}^6$
- P3)**  $\mathbf{D}_\eta(\boldsymbol{\nu}, \boldsymbol{\eta}) > 0, \quad \forall \boldsymbol{\nu}, \boldsymbol{\eta} \in \mathbb{R}^6.$

Note also that the skew-symmetry property of  $\mathbf{C}(\boldsymbol{\nu}, \boldsymbol{\eta})$  does not hold for  $\mathbf{C}_\eta(\boldsymbol{\nu}, \boldsymbol{\eta})$ .

### D. The Pipe Dynamics

The pipe dynamics are modeled by:

$$m_P \ddot{\boldsymbol{\varphi}} = \partial_S \mathbf{n}^e - \mathbf{f}_g^e - \mathbf{R}_t^e \mathbf{f}_D^t \quad (16)$$

$$\mathbf{I}_\rho^e \dot{\mathbf{w}}^e + \mathbf{w}^e \times \mathbf{I}_\rho^e \mathbf{w}^e = \partial_S \mathbf{m}^e + \partial_S \boldsymbol{\varphi} \times \mathbf{n}^e - \mathbf{D}_R \mathbf{w}^e \quad (17)$$

where

- $m_P$  - mass per unit length of the pipe
- $\mathbf{R}_t^e \mathbf{f}_D^t$  - transversal hydrodynamic damping vector
- $\mathbf{n}^e$  - resultant internal force vector
- $\mathbf{f}_g^e$  - restoring force vector
- $\mathbf{I}_\rho^e$  - mass moment of inertia matrix
- $\mathbf{D}_R$  - rotation damping matrix
- $\mathbf{m}^e$  - resultant internal torque vector

and  $\mathbf{D}_R > 0$ . Due to the buoyancy, the restoring forces given as  $\mathbf{f}_g^e = (m_P - \rho_w A) \mathbf{g}^e$ , not only depend on the mass and gravitation  $\mathbf{g}^e = [0, 0, g]^T$ , but also on the mass density of ambient water  $\rho_w$  and the cross-section area of the pipe  $A$ . The damping is estimated using Morison's equation [4] and is given as

$$\mathbf{f}_D^t = \frac{1}{2} d_o \rho_w \mathbf{D}_T \begin{bmatrix} |v_{r_1}^t| v_{r_1}^t \\ \left( (v_{r_2}^t)^2 + (v_{r_3}^t)^2 \right)^{1/2} v_{r_2}^t \\ \left( (v_{r_2}^t)^2 + (v_{r_3}^t)^2 \right)^{1/2} v_{r_3}^t \end{bmatrix} \quad (18)$$

where  $d_o$  is the outer pipe diameter,  $\mathbf{D}_T > 0$  is the damping matrix of translational motion and  $v_{r_i}^t$  are elements of the relative velocity of the pipe in the water,  $\mathbf{v}_r^t = (\mathbf{R}_t^e)^T (\dot{\boldsymbol{\varphi}} - \mathbf{v}_c^e) \in \mathbb{R}^3$ , where  $\mathbf{v}_c^e(\boldsymbol{\varphi}^T \mathbf{e}_3, t)$  is the ocean current velocity at depth  $h + \boldsymbol{\varphi}^T \mathbf{e}_3$ , where  $h$  represents the water depth. Wave excitation forces on the pipe is neglected since they only affect the pipe near to the surface, (typically down to 20m). The time dependent inertia tensor,  $\mathbf{I}_\rho^e(S, t)$ , is given by

$$\mathbf{I}_\rho^e = \mathbf{R}_t^e \mathbf{J}_\rho^t (\mathbf{R}_t^e)^T, \quad \mathbf{J}_\rho^t = \text{diag}[J_1, J_2, J_3] \quad (19)$$

where  $\mathbf{J}_\rho^t \in \mathbb{R}^{3 \times 3}$  is the inertia tensor for the cross section in the reference configuration.

Let the lower end of the pipe be clamped to the seabed, tangent to the  $\mathbf{e}_1$ -axis, thus the boundary conditions at  $S = 0$  is given by

$$\boldsymbol{\varphi}(0, t) = \boldsymbol{\varphi}_0 = 0 \quad (20)$$

$$\mathbf{R}_t^e(0, t) = (\mathbf{R}_t^e)_0 = \mathbf{I}_{3 \times 3}, \quad (21)$$

and the pipelay vessel represents the boundary conditions at  $S = L$ , which can explicitly be expressed by inserting (10) into

$$\begin{bmatrix} \mathbf{n}^e|_L \\ \mathbf{m}^e|_L \end{bmatrix} = - \begin{bmatrix} \mathbf{R}_b^e & \mathbf{0}_{3 \times 3} \\ \mathbf{0}_{3 \times 3} & \mathbf{R}_b^e \end{bmatrix} \boldsymbol{\chi} \quad (22)$$

with the initial conditions

$$\mathbf{R}_t^e(L, t_0) = \mathbf{R}_b^e(t_0) (\mathbf{R}_b^t(\beta))^T. \quad (23)$$

### III. CONTROL DESIGN

The stability properties of the system is investigated in this section. Firstly, an input-output passivity check of the pipelay system with the thrusters as the input and the velocity vector as the output is performed, and secondly a stability check of the pipelay system by condition of feedback connection of two passive systems, which are the pipelay vessel with pipeline and the passive thruster controller, is performed.

#### A. Passivity

Let the thruster force of the vessel  $\tau$  be defined as the input, and the output be defined as the vessel speed in the body frame. The total energy of the system  $\mathcal{E}$ , taken as the storage function is given by

$$\mathcal{E} = \mathcal{E}_P + \mathcal{E}_V \geq 0 \quad (24)$$

where  $\mathcal{E}_P$  and  $\mathcal{E}_V$  are the energy of the pipe and vessel respectively. The pipe energy function  $\mathcal{E}_P$  is the sum of kinetic energy  $\mathcal{T}_P$  and potential energy  $\mathcal{U}_P$ ,

$$\mathcal{E}_P = \mathcal{T}_P + \mathcal{U}_P \quad (25)$$

where

$$\mathcal{T}_P = \frac{1}{2} \int_0^L (m_P \langle \dot{\varphi}, \dot{\varphi} \rangle + \langle \mathbf{w}^e, \mathbf{I}_\rho \mathbf{w}^e \rangle) dS, \quad (26)$$

$$\mathcal{U}_P = \int_0^L \Psi(\gamma^t, \omega^t) dS + \int_0^L \langle \mathbf{f}_g^e, \varphi \rangle dS, \quad (27)$$

and the potential energy function  $\Psi$  is given by the quadratic form

$$\Psi(S, \gamma^t, \omega^t) = \frac{1}{2} [(\gamma^t)^T \mathbf{C}_T \gamma^t + (\omega^t)^T \mathbf{C}_R \omega^t], \quad (28)$$

where  $\{\gamma^t, \omega^t\}$  is the strain measure [17], and

$$\mathbf{C}_T = \text{diag}[EA, GA_2, GA_3] > 0, \quad (29)$$

$$\mathbf{C}_R = \text{diag}[GJ, EI_2, EI_3] > 0. \quad (30)$$

The constants  $E$  and  $G$  are interpreted as the Young's modulus and the shear modulus,  $A$  is the cross-sectional area of the pipe,  $A_2$  and  $A_3$  are the effective shear areas,  $\{I_2, I_3\}$  are the principal moments of inertia of the cross-section plane relative to principal axes  $\mathbf{t}_2, \mathbf{t}_3$  of  $\varphi_0$ , and  $J$  is the *Saint Venant* torsional modulus. Equation (28) is only valid for small strains since it does not have proper growth conditions for extreme strains.

The vessel energy function  $\mathcal{E}_V$  is likewise the sum of kinetic energy  $\mathcal{T}_V$  and potential energy  $\mathcal{U}_V$ , given as

$$\mathcal{T}_V = \frac{1}{2} \dot{\boldsymbol{\eta}}^T \mathbf{M}_\eta \dot{\boldsymbol{\eta}} \quad \text{and} \quad \mathcal{U}_V = \mathcal{G}(\boldsymbol{\eta}), \quad (31)$$

where  $\mathcal{G}(\boldsymbol{\eta}) : \mathbb{R}^6 \rightarrow \mathbb{R}$  is a potential function for  $\mathbf{g}_\eta(\boldsymbol{\eta})$ , such that

$$\nabla \mathcal{G} = \mathbf{g}_\eta \quad \Rightarrow \quad \dot{\mathcal{G}}(\boldsymbol{\eta}) = \mathbf{g}_\eta^T(\boldsymbol{\eta}) \dot{\boldsymbol{\eta}}. \quad (32)$$

The time derivative of (24) is given as

$$\dot{\mathcal{E}} = \dot{\mathcal{E}}_P + \dot{\mathcal{E}}_V, \quad (33)$$

where following [9]  $\dot{\mathcal{E}}_P$  is found to be

$$\begin{aligned} \dot{\mathcal{E}}_P &= [\langle \mathbf{n}^e, \dot{\varphi} \rangle]_0^L + [\langle \mathbf{m}^e, \mathbf{w}^e \rangle]_0^L \\ &\quad - \int_0^L (\langle \dot{\varphi}, \mathbf{R}_t^e \mathbf{f}_D^t \rangle + \langle \mathbf{w}^e, \mathbf{D}_R \mathbf{w}^e \rangle) dS \end{aligned} \quad (34)$$

where the two terms of the integral are square damping terms dissipating energy from the system. Without these terms the system is seen to be energy conservative as the energy is only depending on the boundary conditions. The time derivative of  $\mathcal{E}_V$  is readily seen to be

$$\dot{\mathcal{E}}_V = \dot{\boldsymbol{\eta}}^T \mathbf{M}_\eta \ddot{\boldsymbol{\eta}} + \frac{1}{2} \dot{\boldsymbol{\eta}}^T \dot{\mathbf{M}}_\eta \dot{\boldsymbol{\eta}} + \mathbf{g}_\eta^T(\boldsymbol{\eta}) \dot{\boldsymbol{\eta}} \quad (35)$$

$$= \dot{\boldsymbol{\eta}}^T \mathbf{J}^T \boldsymbol{\tau} + \dot{\boldsymbol{\eta}}^T \mathbf{J}^T \boldsymbol{\chi} - \dot{\boldsymbol{\eta}}^T \mathbf{D}_\eta(\boldsymbol{\nu}, \boldsymbol{\eta}) \dot{\boldsymbol{\eta}} \quad (36)$$

where (11) and properties **P2** and **P3** have been applied. Thus

$$\dot{\mathcal{E}}_V \leq \boldsymbol{\nu}^T \boldsymbol{\tau} + \boldsymbol{\nu}^T \boldsymbol{\chi} \quad (37)$$

which implies that to obtain input-output passivity for the vessel  $\boldsymbol{\nu}^T \boldsymbol{\chi}$  must be canceled.

For the boundary condition at  $S = 0$  it is readily seen that

$$\langle \mathbf{n}^e, \dot{\varphi} \rangle|_0 = \langle \mathbf{m}^e, \mathbf{w}^e \rangle|_0 = 0. \quad (38)$$

The remaining terms,  $S = L$ , are the forces and moments on the pipe from the vessel. Summing the time derivatives of the energy for the vessel (36) and pipe (34),

$$\begin{aligned} \dot{\mathcal{E}} &= \boldsymbol{\nu}^T \boldsymbol{\tau} + \boldsymbol{\nu}^T \boldsymbol{\chi} - \dot{\boldsymbol{\eta}}^T \mathbf{D}_\eta(\boldsymbol{\nu}, \boldsymbol{\eta}) \dot{\boldsymbol{\eta}} \\ &\quad + \langle \mathbf{n}^e, \dot{\varphi} \rangle|_L + \langle \mathbf{m}^e, \mathbf{w}^e \rangle|_L \end{aligned} \quad (39)$$

$$- \int_0^L (\langle \dot{\varphi}, \mathbf{R}_t^e \mathbf{f}_D^t \rangle + \langle \mathbf{w}^e, \mathbf{D}_R \mathbf{w}^e \rangle) dS \quad (40)$$

and it is readily seen by inserting (22), and noting that

$$\boldsymbol{\nu} = \begin{bmatrix} \mathbf{v} \\ \boldsymbol{\omega} \end{bmatrix} = \begin{bmatrix} \mathbf{R}_e^b \dot{\varphi} \\ \mathbf{R}_e^b \mathbf{w}^e \end{bmatrix}, \quad (41)$$

the forces and moments acting between the vessel and the pipe cancel so that (39) reduces to

$$\begin{aligned} \dot{\mathcal{E}} &= \boldsymbol{\nu}^T \boldsymbol{\tau} - \dot{\boldsymbol{\eta}}^T \mathbf{D}_\eta(\boldsymbol{\nu}, \boldsymbol{\eta}) \dot{\boldsymbol{\eta}} \\ &\quad - \int_0^L (\langle \dot{\varphi}, \mathbf{R}_t^e \mathbf{f}_D^t \rangle + \langle \mathbf{w}^e, \mathbf{D}_R \mathbf{w}^e \rangle) dS \end{aligned} \quad (42)$$

where the properties of the damping terms are known from the previous sections such that  $\dot{\mathcal{E}} \leq \boldsymbol{\nu}^T \boldsymbol{\tau}$ , and input-output passivity from thruster force to vessel motion of the total system has been shown.

#### B. Controller

An important objective in the competitive pipelay industry is to improve the profit margins by optimize the utilization of the equipment by increasing the operational time of the vessel and also to reduce the cost of pipe path preparation on the seabed. The tension from the pipe on the vessel is a function of the water depth, pipe density and bending stiffness, and must be counteracted by the vessel thrusters

to obtain a desired pipe configuration. Low tension yields a steep configuration where the touchdown point is located close to the vessel, which reduces free spans and allows for smaller radii of the pipe on the seabed and thus reduces the need for seabed preparation as the pipe can more easily be placed to avoid obstacles. Also advocating for low tension is the directly proportional relationship to the fuel cost [10]. However, too little tension will cause the pipe string to buckle, which occurs when the strain exceeds the pipe design limit and collapses. Finding the optimal tension is an optimization task where the above issues are considered.

A simple and common control strategy is *tension control* which is based on the measured tension of the pipe at the vessel. In this paper a controller is designed to shape the configuration of the pipe. Assume that a desired pipe configuration  $\varphi_{ref}$  is known. This may typically be obtained from simulations in tools like SIMLA. There exists a mapping  $\mathbf{F}$  from the desired configuration to desired vessel position  $\boldsymbol{\eta}_{ref}$  and velocities  $\boldsymbol{\nu}_{ref}$ ;

$$\mathbf{F} : (\varphi_{ref}, \mathbf{R}_t^e) \rightarrow (\boldsymbol{\eta}_{ref}, \boldsymbol{\nu}_{ref}) \quad (43)$$

Known measurements are the vessel and touchdown point positions and attitudes, the pipe tension at the vessel, the length of the suspended pipe and the stinger configuration for S-lay. In practical applications, the external environmental forces of wind, waves and current must be accounted for in the controller, so the nonlinear PID-controller is suggested

$$\boldsymbol{\tau} = -\mathbf{J}^T(\boldsymbol{\eta}) \boldsymbol{\tau}_{PID} \quad (44)$$

$$\boldsymbol{\tau}_{PID} = \mathbf{K}_p \tilde{\boldsymbol{\eta}} + \mathbf{K}_d \dot{\tilde{\boldsymbol{\eta}}} + \mathbf{K}_i \int_{t_0}^t \tilde{\boldsymbol{\eta}}(\tau) d\tau \quad (45)$$

where  $\tilde{\boldsymbol{\eta}} = \boldsymbol{\eta} - \boldsymbol{\eta}_{ref}$ , and the matrices  $\mathbf{K}_p, \mathbf{K}_d, \mathbf{K}_i \in \mathbb{R}^{6 \times 6}$  are controller gains. It is assumed that a wave filter removes the 1<sup>st</sup> order waves, and the effect of wind is handled as a feed-forward term. The integrator term removes the bias caused by current and 2<sup>nd</sup> order waves. Assuming the vessel to be fully actuated, the available control input are the vessel thrusters, which are limited to surge, sway and yaw. By choosing a passive controller such as a PD-controller ( $\mathbf{K}_i = \mathbf{0}$ ), the closed loop system is stable by the condition of feedback connection of two passive systems, found in Theorem 6.1 in [11]. However, this property is generally not guaranteed for the PID-controller due to the integrator term, unless the integral action term of the controller is bounded.

#### IV. SIMULATIONS

A standard Galerkin finite element method, with linear shape functions, is applied on (16–17) with (20–22) as boundary conditions. The integration in time is handled by the embedded Matlab ODE-solver `ode15s`, suitable for stiff systems, with the timestep set to 0.03s. To find the static equilibrium configuration, a Newton Raphson iterative scheme [19] is applied to the linearized weak formulation of the static model. Integrals are approximated by using Gauss-quadrature. A linearized model of the vessel (10) found in *GNC Toolbox* [6] is used for the pipelay vessel.

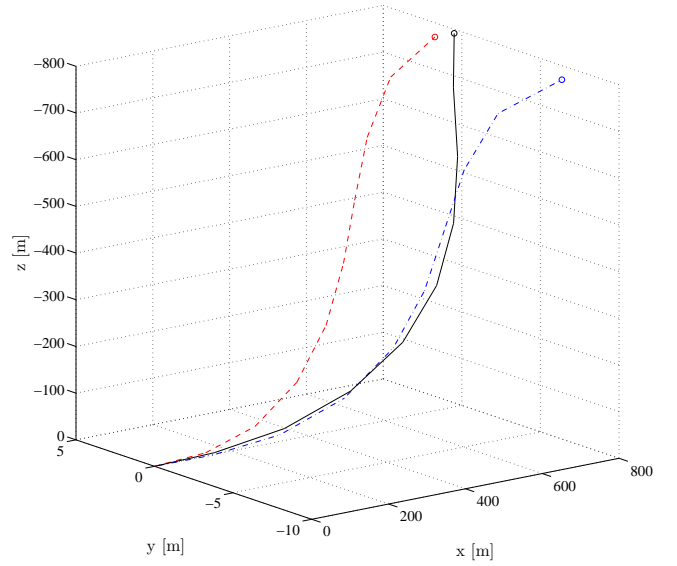


Fig. 2. The dashed red line is the initial static configuration. Dash dot blue line is at  $t = 30s$  where the controller is turned on. Solid black line is configuration at  $t = 200s$ .

The position of the vessel in the static equilibrium is computed to be  $\boldsymbol{\eta}_0 = [729.96, 0, -800.38, 0, 0.13, 0]^T$  based on the following parameters:

$$\begin{aligned} \mathbf{R}_b^t &= \mathbf{I}_{3 \times 3} & \boldsymbol{\eta}_{ref} &= [780, 0, 0, 0, 0, 0]^T \\ n &= 10 & \mathbf{w} &= [0, 6 \cdot 10^5, 0, 0, 0, 0]^T \\ h &= 800\text{m} & \mathbf{J} &= 10^2 \cdot \text{diag}[1, 1, 2]^T \\ L &= 1200\text{m} & \mathbf{C}_T &= 10^9 \cdot \text{diag}[1, 1, 1]^T \\ d_i &= 0.57\text{m} & \mathbf{C}_R &= 10^{11} \cdot \text{diag}[1, 1, 1]^T \\ d_o &= 0.60\text{m} & \mathbf{D}_T &= 1.5 \cdot \text{diag}[1, 1, 1]^T \\ \boldsymbol{\beta} &= [0, 0, 0]^T & \mathbf{D}_R &= 1.5 \cdot \text{diag}[1, 1, 1]^T \\ \rho_a &= 1.200 \cdot 10^3 \text{g/m}^3 & \rho &= (\rho_a - \rho_s) (d_i/d_o)^2 + \rho_s \\ \rho_w &= 1.025 \cdot 10^6 \text{g/m}^3 & \rho_s &= 7.850 \cdot 10^6 \text{g/m}^3. \end{aligned}$$

The course of the simulation is as follows. The pipe starts in the static equilibrium. At time  $t = 10 s$  the environmental forces on the vessel  $\mathbf{w}$  and linearly shared current velocity profile with surface velocity 0.8 m/s in the  $-y$  direction is applied. At time  $t = 30 s$  the controller is turned on. The configurations at the different times are illustrated in Figure 2, and Figure 3 show the elements of  $\boldsymbol{\eta}$  for the vessel when the PD-controller is applied with the following controller gains:

$$\mathbf{K}_p = \text{diag}[0.5 \cdot 10^6, 0.5 \cdot 10^6, 0, 0, 0, 0]^T \quad (46)$$

$$\mathbf{K}_d = \text{diag}[0.4 \cdot 10^7, 0.4 \cdot 10^7, 0, 0, 0, 0]^T. \quad (47)$$

In Figure 4 a PID-controller has been applied with the following controller gains:

$$\mathbf{K}_p = \text{diag}[0.4 \cdot 10^6, 0.4 \cdot 10^6, 0, 0, 0, 10^5]^T \quad (48)$$

$$\mathbf{K}_d = \text{diag}[0.5 \cdot 10^7, 0.4 \cdot 10^7, 0, 0, 0, 10^5]^T \quad (49)$$

$$\mathbf{K}_i = \text{diag}[0.1 \cdot 10^4, 0.5 \cdot 10^4, 0, 0, 0, 0.2 \cdot 10^4]^T. \quad (50)$$

Applying a PID-controller removes the bias seen in the PD-controller simulation.

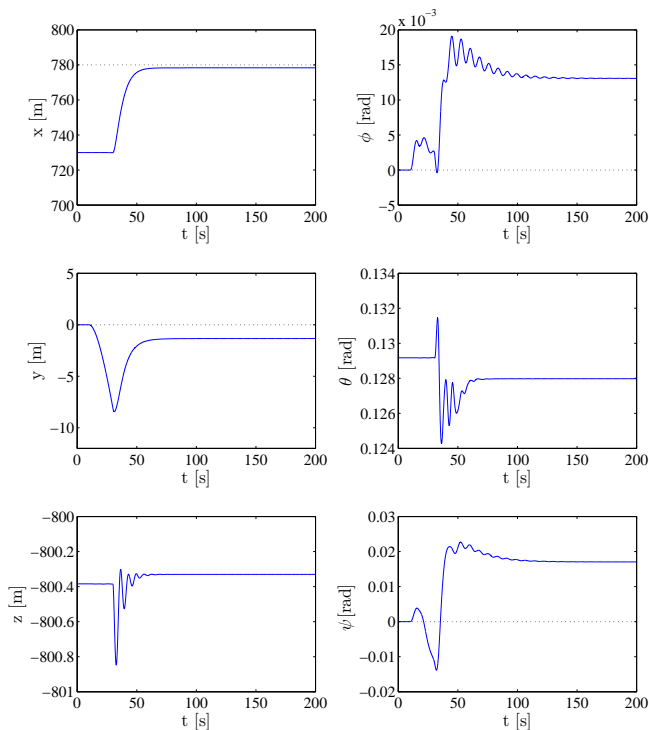


Fig. 3. Postion and orientation of  $\eta$  over the course of the simulation. The PD-controller is enabled at  $t = 30s$ . The dotted line indicates  $\eta_{ref}$  for the controlled states. Note the bias.

## V. CONCLUSIONS

A mathematical model suitable for pipelay operations from a dynamically positioned surface vessel has been presented in this paper. The pipe string has been modeled by a nonlinear dynamic formulation in three dimensions capable of undergoing shearing, twist, and bending. A nonlinear model of the pipelay vessel has been taken as the upper boundary condition for solving the numerical problem. The pipelay system has been shown to be passive taking the thruster force as input and the vessel velocity as the output. A nonlinear controller considering the kinematics is presented and applied in numerical simulations to illustrate the theoretical results. For future extensions of the pipe model, seabed and stinger interaction forces should be added to the model, and the pipe length should be made a function of time  $L(t)$  to handle pay-out of pipe from the vessel.

## REFERENCES

- [1] M. J. Balas. Active control of flexible systems. *Journal Of Optimization Theory And Applications*, 25(3):415–436, 1978.
- [2] M. W. Braestrup, J. B. Andersen, L. W. Andersen, M. B. Bryndum, C. J. Christensen, and N. Rishy. *Design and Installation of Marine Pipelines*. Blackwell Science Ltd, 2005.
- [3] D. Dixon and D. Rutledge. Stiffened catenary calculations in pipeline laying problem. *ASME Journal of Engineering for Industry*, (90):153–160, February 1968.
- [4] O. M. Faltinsen. *Sea Loads on Ships and Offshore Structures*. Cambridge University Press, 1990.
- [5] T. I. Fossen. *Marine Control Systems: Guidance, Navigation, and Control of Ships, Rigs and Underwater Vehicles*. Marine Cybernetics, Trondheim Norway, 1st edition, 2002.
- [6] T. I. Fossen and T. Perez. Marine systems simulator (MSS). ([www.marinecontrol.org](http://www.marinecontrol.org)), 2004.

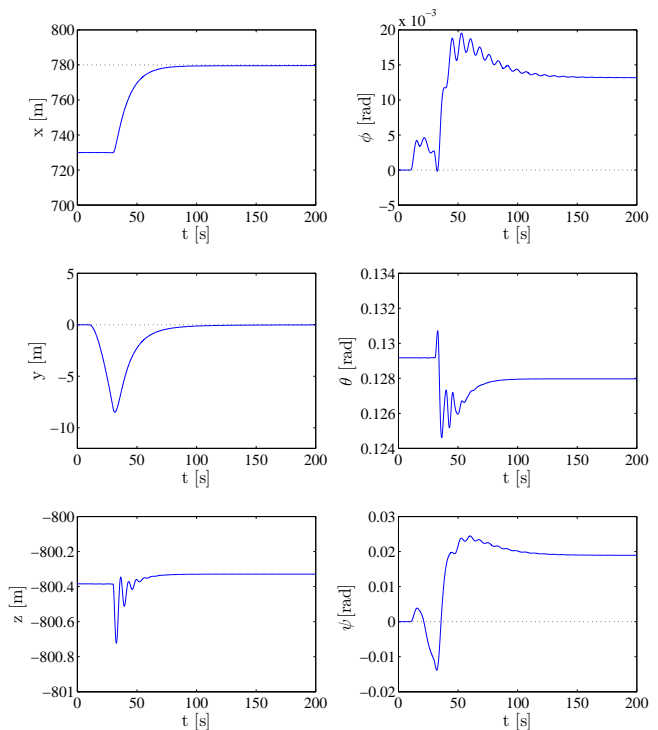


Fig. 4. Postion and orientation of  $\eta$  over the course of the simulation. The PID-controller is enabled at  $t = 30s$ . The dotted line indicates  $\eta_{ref}$  for the controlled states. Note that the integrator term cancels the bias terms seen when the PD-controller was applied.

- [7] B. Guo, S. Song, J. Chacko, and A. Ghalambor. *Offshore Pipelines*. Gulf Professional Publishing, 2005.
- [8] E. Heerema. Recent achievements and present trends in deepwater pipe-lay systems. In *Proceedings of the 37th Offshore Technology Conference*, 2005. OTC 17627.
- [9] G. A. Jensen. *Modeling and Control of Offshore Pipelay Operations*. PhD thesis, Norwegian University of Science and Technology, 2009.
- [10] M. Kashani and R. Young. Installation load consideration in ultra-deepwater pipeline sizing. *Journal of Transportation Engineering*, 131(8):632–639, Aug. 2005.
- [11] H. Khalil. *Nonlinear Systems*. Prentice Hall, 3rd edition, 2002.
- [12] R. Knight and O. Palathingal. Pipelay market constrained by vessel shortages? In *OTC07 Show Daily 05.02.07*, pages 20–21, 2007.
- [13] S. Kyriakides and E. Corona. *Mechanics of Offshore Pipelines, Volume 1: Buckling and Collapse*. Elsevier, 1 edition, 2007.
- [14] A. C. Palmer and R. A. King. *Subsea Pipeline Engineering*. PennWell Books, 2nd edition, 2008.
- [15] D. Perinet and I. Frazer. J-lay and Steep S-lay: Complementary tools for ultradeep water. In *Proceedings of the 39th Offshore Technology Conference*, 2007. OTC 18669.
- [16] R. Plunkett. Static bending stresses in catenaries and drill strings. *Journal of Engineering for Industry*, February 1967.
- [17] J. C. Simo. A finite strain beam formulation. The three-dimensional dynamic problem. Part I. *Computer Methods in Applied Mechanics and Engineering*, 49(1):55–70, May 1985.
- [18] J. C. Simo, N. Tarnow, and M. Doblare. Non-linear dynamics of three-dimensional rods: Exact energy and momentum conserving algorithms. *International Journal For Numerical Methods in Engineering*, 38:1431–1473, 1995.
- [19] J. C. Simo and L. Vu-Quoc. A three-dimensional finite-strain rod model. Part II: Computational aspects. *Computer Methods in Applied Mechanics and Engineering*, 58(1):79–116, Oct. 1986.
- [20] J. C. Simo and L. Vu-Quoc. On the dynamics in space of rods undergoing large motions – a geometrically exact approach. *Computer Methods in Applied Mechanics and Engineering*, 66(2):125–161, Feb. 1988.